Supplementary Information

Modular Assembly of Arterial Organoids Enables Rapid Blood Perfusion to Ameliorate Ischemic Diseases

Weijing Kong(孔维静)[1,2,#], Zihang Pan(潘子航)[1,2,3,#,*], Yi Hong(洪毅)[1,2], Liangliang Tian(田亮亮)[1,2], Qiyang Yao(姚启扬)[1,2], Yun Zhao(赵云)[1,2], Zixuan Hong(洪子玹)[1,2], Xiaojing Ma(马潇菁)[1,2], Simin Jiang(蒋思敏)[1,2], Dayan Li(李大雁)[1,2], Yuxuan Guo(郭宇轩)[3], Xiaoxia Li(李肖霞)[1,2], Lijun Sun(孙立君)[1,2], Jiao Liu(刘皎)[4], Qijia Liu(刘启佳)[5], Erdan Dong(董尔丹)[2,3,6,7], Jing Liu(刘静)[8], Rica Tanaka[9], Jiaxuan Feng(冯家烜)[10], Tao Zhang(张韬)[11], Xi Wang(王茜)[1,12*], Kai Wang(王凯)[1,2,13*]

Inventory of Supplementary Information

1. Supplementary Tables, Contains:

2. Supplementary Figures S1-S8, Supplementary Figure Legends

Supplementary Table 1. List of primary antibodies used for immunofluorescence staining and Western blotting

Antigen	Manufacturer	Catalog #	Dilution	Application
Anti-CD144	Santa Cruz	sc-58707	1:100	IF
Anti-CD31	Santa Cruz	sc-53411	1:100	IF
Anti-PDGFRβ	R&D systems	AF385	1:200	IF
Anti-CollagenIV	Abcam	ab214417	1:200	IF
Anti-CXCR4	Abcam	ab181020	1:200	IF
Anti-Podocalyxin	R&D systems	AF1658	1:200	IF
Anti-SOX17	R&D systems	AF1924	1:500	IF, IHC-P
Anti-CD31	R&D systems	AF806	1:200	IHC-P
Anti-α-SMA	Santa Cruz	sc-32251	1:200	IHC-P
Anti-α-SMA	Abcam	ab5694	1:200	IHC-P
Anti-Vimentin (V9)	Santa Cruz	sc-6260	1:100	IHC-P
Anti-KU80	Cell Signaling Technology	2180S	1:200	IHC-P
Anti-F4/80	ABclonal	A23788	1:200	IHC-P
Anti-COUP-TFII	Abcam	ab211776	1:200	IHC-P
Anti-CD144	Abcam	ab33168	1:1000	WB
Anti-ETV2	Abcam	ab181847	1:1000	WB
Anti-TAL1	Abcam	ab155195	1:1000	WB
Anti-GAPDH	ZSGB-Bio	TA-08	1:1000	WB

Supplementary Table 2. List of primary antibodies used for flow cytometry

Antigen	Manufacturer	Catalog #	Dilution
FITC-CD31	Biolegend	303104	1:100
APC-CD31	Biolegend	303116	1:100
PE-CD31	Biolegend	303106	1:100
APC-DLL4	Biolegend	MD4-46	1:100
FITC-CD11b	Biolegend	101205	1:100
PE-CD11b	Biolegend	101207	1:100
APC-mouse CD45	Biolegend	103112	1:100
PE-mouse F4/80	Biolegend	123110	1:100
BV421-mouse CD11c	Biolegend	117329	1:100
APC-mouse CD335	Biolegend	137607	1:100
APC/Cyanine7-mouse Ly-6G	Biolegend	127623	1:100
BV650-mouse F4/80	Biolegend	123149	1:100
BV785-mouse Ly-6C	Biolegend	128041	1:100
APC/Fire 810-mouse Ly-6G/LY-6C	Biolegend	108469	1:100
TruStain FcX PLUS	Biolegend	156603	1:100
BUV395-mouse CD45	BD Biosciences	565967	1:100
PE-Cy7-mouse CD19	BD Biosciences	561739	1:100
PE-mouse I-A/I-E	BD Biosciences	562010	1:100
PE-CD144	Thermo Fisher	12-1449-82	1:100

Supplementary Table 3. List of chemicals, peptides and recombinant proteins

Reagent	Manufacturer	Catalog #
mTeSR medium	STEMCELL Technologies	85851, 85852
Penicillin/streptomycin	Thermo Fisher	15-140-122
PureCol EZ Gel solution	Sigma	5074
TrypLE Express Enzyme (1X)	Thermo Fisher	12604013
Trypsin-EDTA, 0.05%	Thermo Fisher	25300054
Advanced DEME/F-12	Thermo Fisher	12634028
DMEM/F12	Thermo Fisher	c11330500bt
RPMI 1640	Thermo Fisher	11875119
Recombinant human VEGFA	Sino Biological	11066-HNAH
Recombinant human FGF2	Sino Biological	10014-HNAE
Recombinant human EGF	Sino Biological	10605-HNAE
FITC-Dextran (70 KDa)	Beyotime	ST2947
Cy5-Dextran (70 KDa)	Yusi Pharmaceutical	YS-De1623
CHIR99021	Topsciencepi	T2310
SB431542	Topscience	T1726
Y-27632 dihydrochloride	Topscience	T1870
D-luciferin, Potassium Salt	Vazyme	DD1210
L-ascorbic acid	Sigma	A8960

Reagent	Manufacturer	Catalog #
Glutamax	Thermo Fisher	35050061
Bovine serum albumin (BSA)	Sigma	A2153
RIPA Lysis Buffer	Beyotime	P0013B
10% Formalin	Sigma	F5554
Recombinant Human TNF-a	Novoprotein	C008
Triton X-100	Sigma	X100-500ML
PBS, pH7.4	Corning	21-040-CV
DAPI solution	Solarbio	C0060
Fetal Bovine Serum (FBS)	Thermo Fisher	10099158
FACS Stain Buffer	BD Biosciences	554657
RBC Lysis Buffer	Biolegend	420301
Brilliant Stain Buffer	Thermo Fisher	00-4409-75
Sealed horse serum	ZSGB-BIO	ZLI-9024
Collagenase, Type I	Thermo Fisher	17018029
Collagenase, Type II	Thermo Fisher	17101015
Collagenase, Type IV	Thermo Fisher	17104019
Dispase II	Thermo Fisher	17105041
FemtoLight ECL	Epizyme	SQ201
10% SDS-PAGE gels	Epizyme	P0690
Matrigel Matrix Growth Factor Reduced (GFR)	Corning	356231

Reagent	Manufacturer	Catalog #
Lycopersicon Esculentum Lectin DyLight 649	Thermo Fisher	L32472
EDTA Antigen Retrieval Solution (pH 8.0)	Solarbio	C1033
Fluoroshield Mounting Medium With DAPI	Abcam	ab104139
Clodronate Liposomes & Control Liposomes	LIPOSOMA	CP-005-005

Supplementary Figures

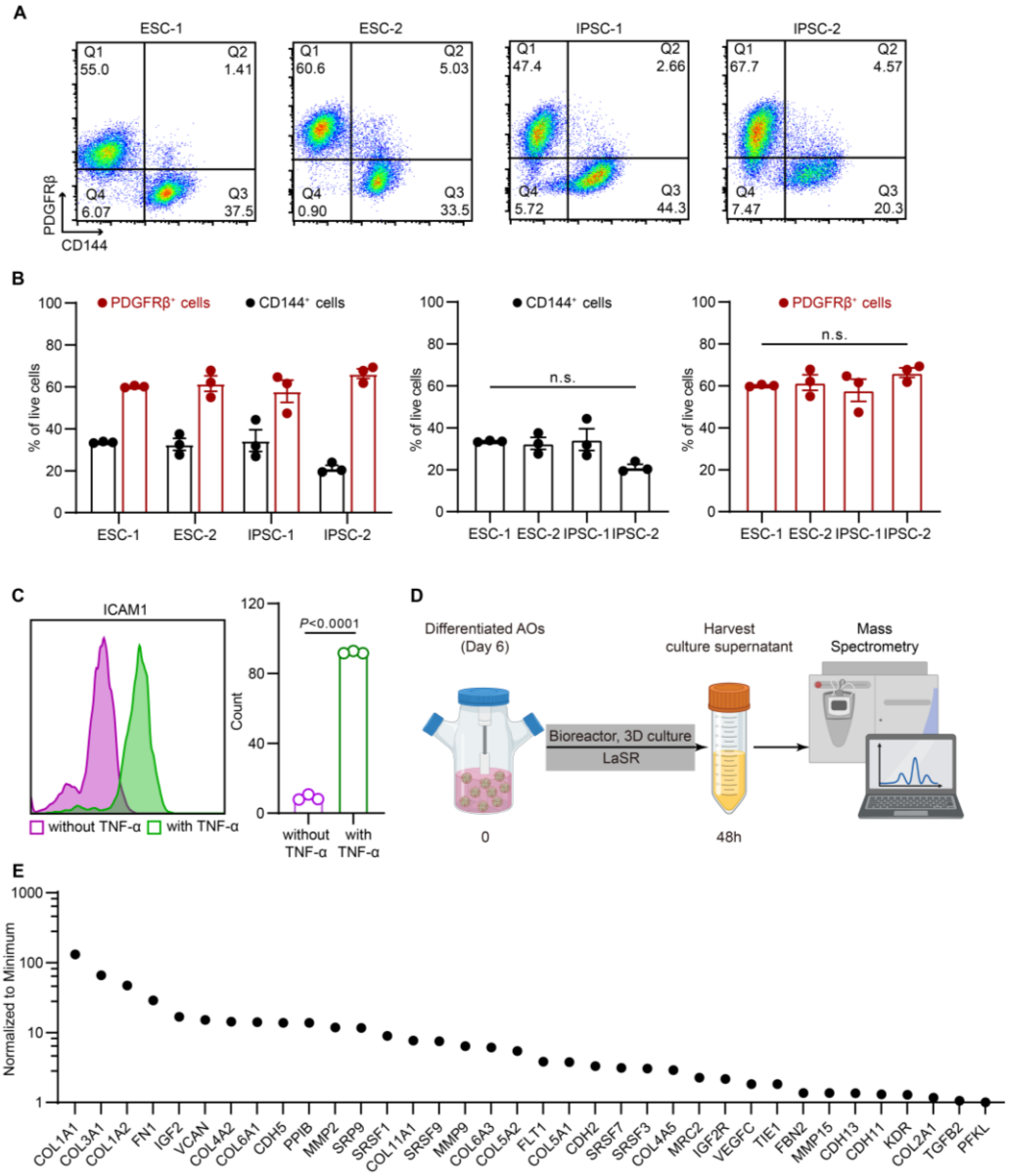

Figure S1. Reproducibility of AOs differentiation across independent pluripotent stem cell lines. (**A**) Representative flow cytometry plots showing CD144⁺ ECs and PDGFRβ⁺ MCs in AOs generated from two human ESC and two human iPSC lines. (**B**) Quantification of CD144⁺ ECs and PDGFRβ⁺ MCs proportions across independent differentiation batches. *n* = 3 independent

differentiation experiments. One-way ANOVA with Tukey's post hoc test was performed. (**C**) AOs were treated with or without TNF-α, and ICAM1 expression on ECs was quantified by flow cytometry. n = 3 independent flow cytometry experiments. Two-tailed Student's t-test was used to compare the two groups. Data are presented as mean ± s.e.m. Significance is indicated as n.s., not significant; * $P < 0.05$; ** $P < 0.01$; and *** $P < 0.001$. (**D**) Schematic representation of the experimental workflow. Graphical elements were created in BioRender. Wang, K. (2026) https://BioRender.com/ixkg86f, and the figure was assembled by Adobe Illustrator. (**E**) Mass spectrometry analysis of the paracrine secretome of AOs. Source data, including exact P values, are provided in the Source Data file.

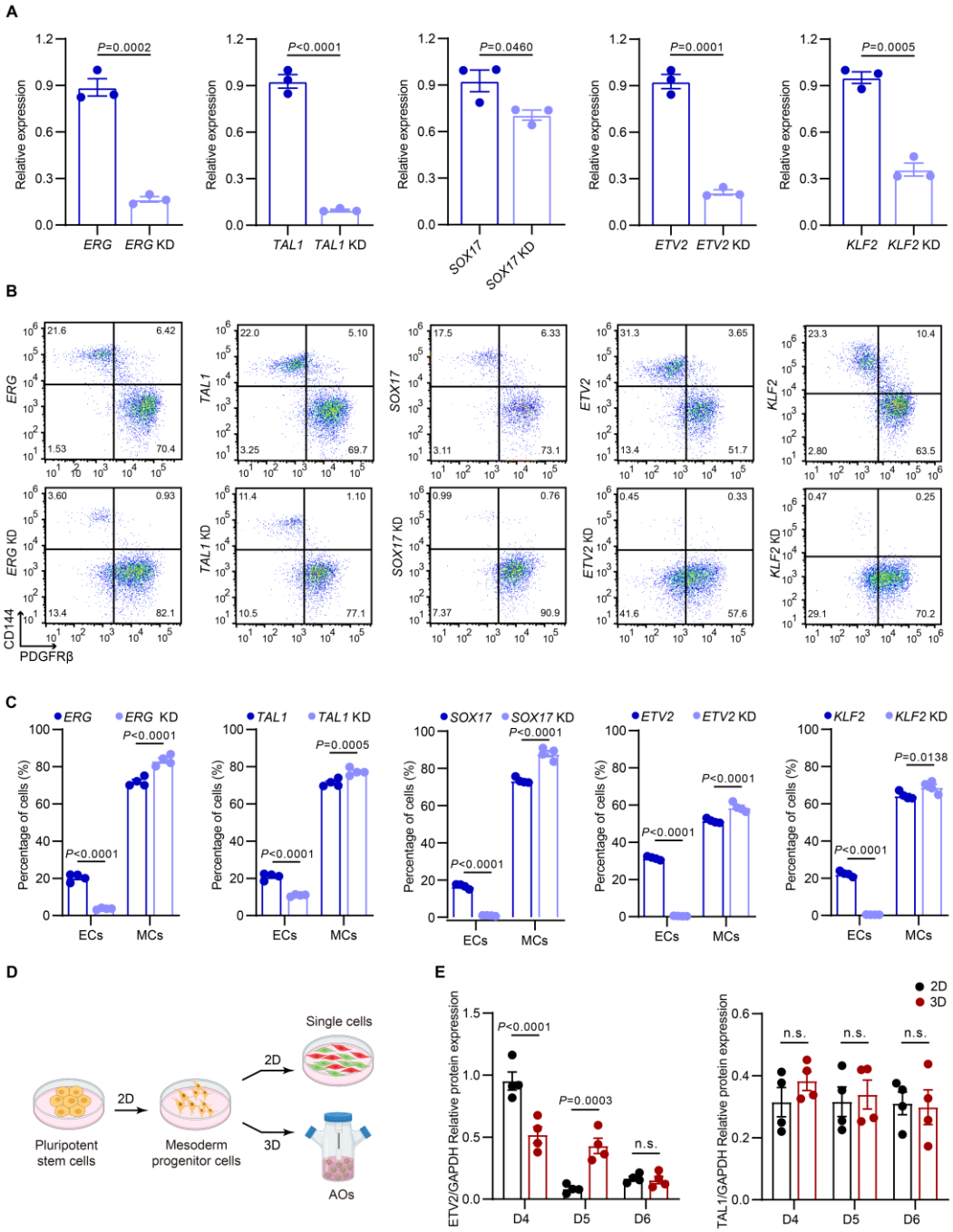

Figure S2. Transcriptional regulation during AOs specification. (**A**) qPCR analysis confirming knockdown efficiency of SOX17, TAL1, KLF2, ERG, and ETV2 in iPSCs. Gene expression levels were normalized to GAPDH and presented relative to the control group. *n* = 3 independent experiments. Two-

tailed Student's *t*-test was used to compare the two groups. (**B**) Representative flow cytometry plots showing the proportions of $CD144^+$ ECs and $PDGFR\beta^+$ MCs in AOs derived from control and transcription factor-knockdown iPSCs. (**C**) Quantification of flow cytometry results shown in (B). Two-way ANOVA with Bonferroni post-hoc test was performed. (**D**) Schematic illustration of the experimental design comparing 3D AOs and 2D single cells differentiated under identical protocols. Graphical elements were created in BioRender. Wang, K. (2026) https://BioRender.com/552r726, and the figure was assembled by Adobe Illustrator. (**E**) Quantification of ETV2 and TAL1 expression normalized to GAPDH. $n = 4$ independent western blot experiments. Two-way ANOVA with Bonferroni post-hoc test was performed. Data are presented as mean ± s.e.m. Significance is indicated as n.s., not significant; *$P < 0.05$; ** $P < 0.01$; and *** $P < 0.001$. Source data, including exact P values, are provided in the Source Data file.

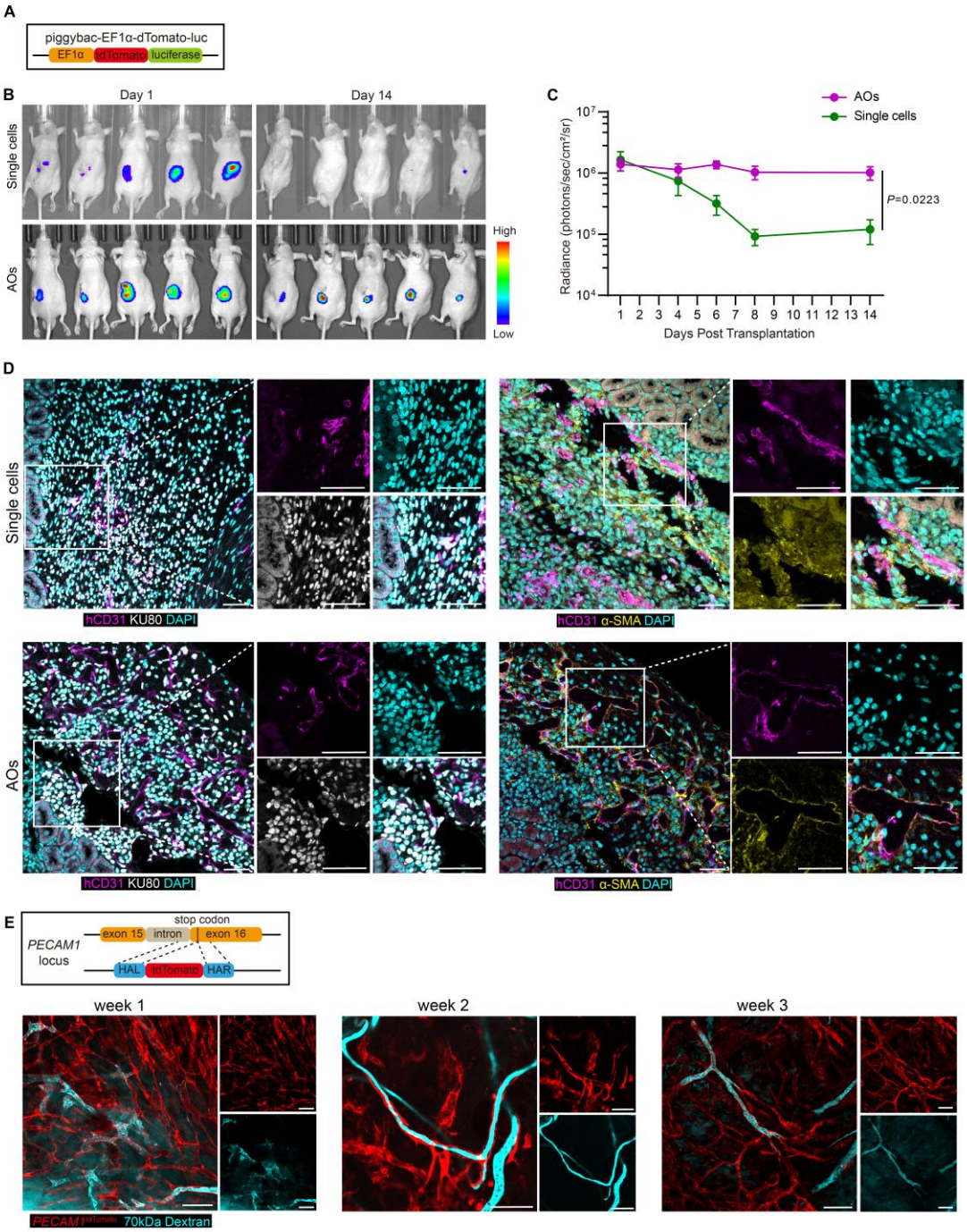

Figure S3. Visualization and quantitative analysis of graft survival and vascular network formation. (**A**) Schematic of the luciferase-expressing transgene (piggyBac-EF1α-tdTomato-luc) used for *in vivo* bioluminescence tracking of transplanted cells. (**B**) Bioluminescent imaging of mice transplanted

with single cells or AOs on days 1 and 14. (**C**) Quantification of bioluminescence intensity from single cells and AOs grafts. n = 5 mice. Two-way ANOVA with Bonferroni post-hoc test was performed. Data are presented as mean ± s.e.m. Significance is indicated as n.s., not significant; * $P < 0.05$; ** $P < 0.01$; and *** $P < 0.001$. (**D**) Immunofluorescent staining of kidney graft sections 14 days after transplantation. Upper panels: single cells group; lower panels: AOs group. Staining for human nuclear antigen ($KU80^+$, white), human ECs ($CD31^+$, magenta), MCs (α-SMA^+, yellow), and nuclei counterstained with DAPI (cyan). Scale bar: 50 μm. (**E**) Schematic of genome-editing strategy used to generate a reporter iPSC line targeting PECAM1 loci. Representative perfused AOs-derived vascular structures were visualized following intravenous injection of 70 kDa dextran (cyan). Scale bar: 100 μm. Source data, including exact P values, are provided in the Source Data file.

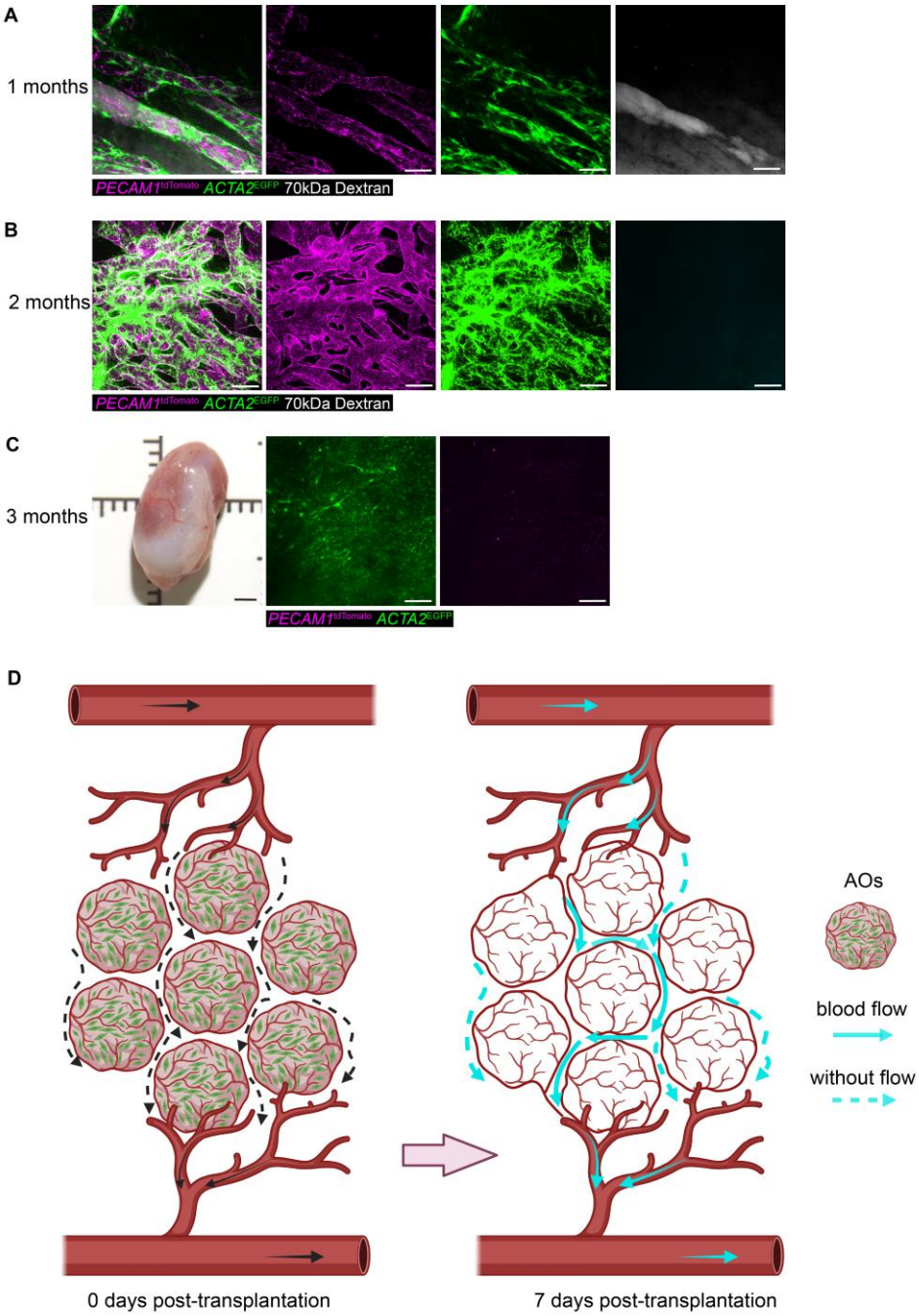

Figure S4. Long-term evaluation of AOs-derived vascular structures following kidney capsule transplantation. Representative intravital confocal microscopy images of AOs-derived vascular structures 1 month (**A**), 2 months (**B**) and 3 months (**C**) after transplantation under the kidney capsule. Scale bar:

100 μm in fluorescence images and 2 mm in gross images. (**D**) Schematic illustration of AOs modular assembly and vascular network formation. Graphical elements were created in BioRender. Wang, K. (2026) https://BioRender.com/0isw1hn, and the figure was assembled by Adobe Illustrator.

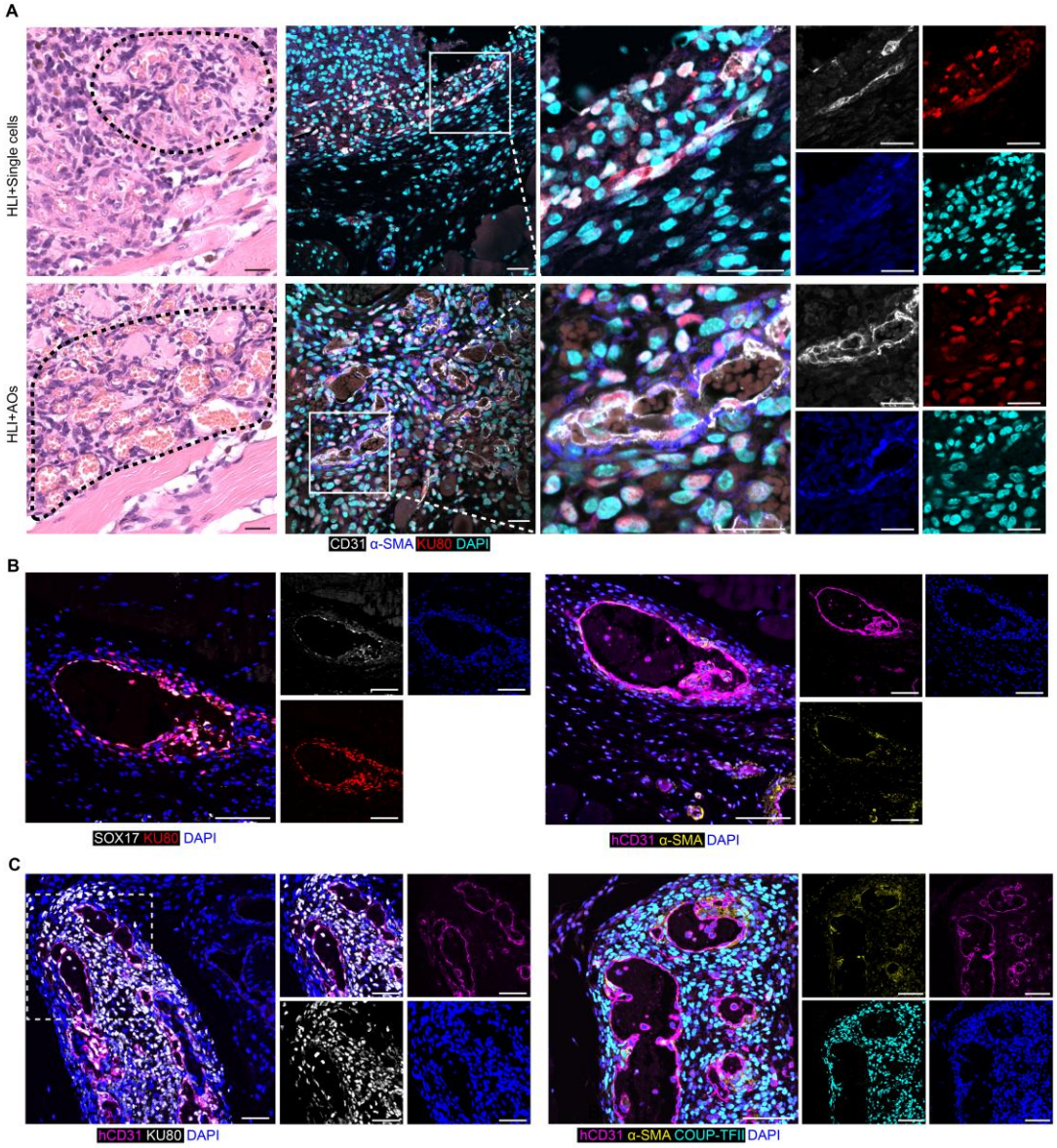

Figure S5. Tissue architecture and vascular characterization of AOs grafts in ischemic hindlimb muscles. (**A**) Representative H&E staining (left panels) and immunofluorescence (middle and right panels) of ischemic hindlimb muscles harvested 14 days after transplantation. Black dashed boxes indicate representative graft-associated areas selected for evaluation of local tissue architecture and fibrosis. Immunostaining for ECs ($CD31^+$, white), MCs (α-SMA^+, blue), human nuclear antigen ($KU80^+$, red), and nuclei counterstained

with DAPI (cyan). Scale bar: 25 μm. (**B**) Representative immunofluorescence images showing expression of the arterial-associated marker in human-derived vascular structures following AOs transplantation. Staining for arterial marker ($SOX17^+$, white), human nuclear antigen ($KU80^+$, red), human ECs ($CD31^+$, magenta), MCs (α-SMA^+, yellow), and nuclei counterstained with DAPI (blue). Scale bar: 200 μm. (**C**) Representative immunofluorescence images showing expression of the venous marker in human-derived vascular structures following AOs transplantation. Staining for venous marker ($COUP\text{-}TFII^+$, cyan), human nuclear antigen ($KU80^+$, white), human ECs ($CD31^+$, magenta), MCs (α-SMA^+, yellow), and nuclei counterstained with DAPI (blue). Scale bar: 100 μm.

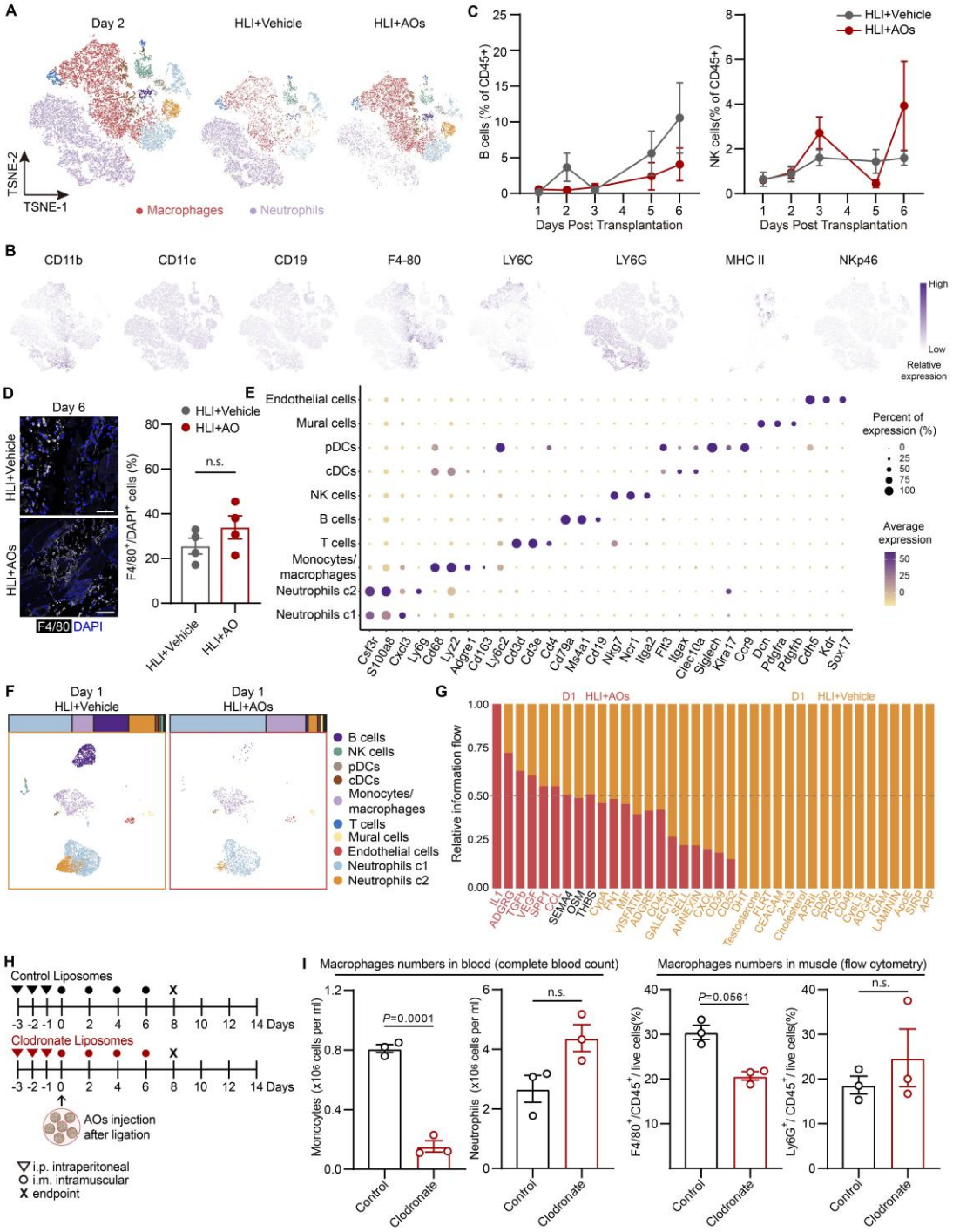

Figure S6. Immune profiling and macrophage depletion analysis in AOs-treated ischemic muscles. (**A**) t-SNE visualization of immune cell populations from ischemic muscle single-cell suspensions after AOs or vehicle treatment, based on flow cytometry analysis. (**B**) t-SNE visualization showing marker expression patterns across immune cell populations. (**C**) Temporal dynamics

(days 1 - 6) of B cells and NK cells following AOs or vehicle treatment in ischemic muscles. *n* = 3 mice. Two-way ANOVA with Bonferroni post-hoc test was performed. (**D**) Representative immunofluorescence staining of ischemic muscle tissue showing macrophages ($F4/80^+$, white) and nuclei counterstained with DAPI (cyan). Scale bar: 50 μm. *n* = 4 mice. Two-tailed Student's *t*-test was used to compare the two groups. (**E**) Dot plot of canonical marker gene expression across identified cell populations. (**F**) UMAP plots depicting cellular clustering of ischemic muscle tissue at day 1 after AOs or vehicle treatment. (**G**) Comparison of signaling pathway activity between the two groups. (**H**) Schematic diagram of the experimental timeline. Graphical elements were created in BioRender. Wang, K. (2026) https://BioRender.com/2e8f6ee, and the figure was assembled by Adobe Illustrator. (**I**) Quantification of monocytes and neutrophils in mouse peripheral blood (left) by complete blood count (CBC) and in local muscle tissue (right) by flow cytometry, both performed 3 days after macrophage depletion treatment. *n* = 3 mice. Two-tailed Student's *t*-test was used to compare the two groups. Data are presented as mean ± s.e.m. Significance is indicated as n.s., not significant; * $P < 0.05$; ** $P < 0.01$; and *** $P < 0.001$. Source data, including exact *P* values, are provided in the Source Data file.

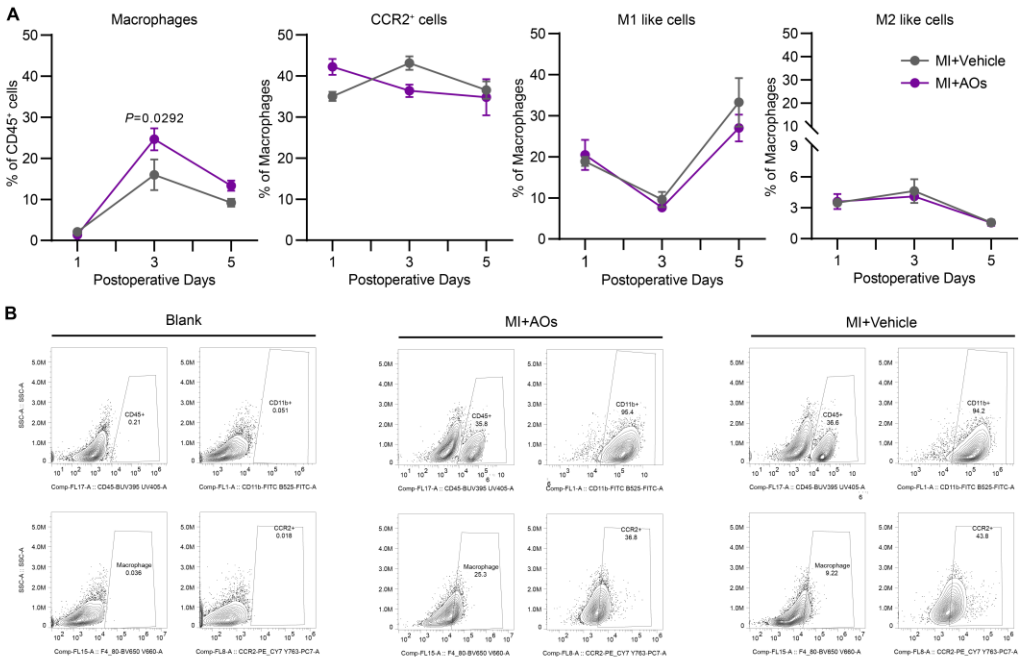

Figure S7. AOs transplantation regulates macrophage responses after myocardial infarction. (**A**) Flow cytometric quantification of total macrophages, CCR2$^+$ macrophages, and macrophage subsets with inflammatory-like or reparative-like signatures in infarcted hearts collected at days 1, 3, and 5 after AOs transplantation or vehicle treatment. n = 3 mice. Two-way ANOVA with Bonferroni post-hoc test was performed. Data are presented as mean ± s.e.m. Significance is indicated as n.s., not significant; *P < 0.05; **P < 0.01; and ***P < 0.001. (**B**) Representative flow cytometry plots from Blank, MI+Vehicle, and MI+AOs groups at day 3 after myocardial infarction. Cardiac immune cells were sequentially gated as CD45$^+$ leukocytes, CD11b$^+$ myeloid cells, F4/80$^+$ macrophages, and CCR2$^+$ macrophages. Source data, including exact P values, are provided in the Source Data file.

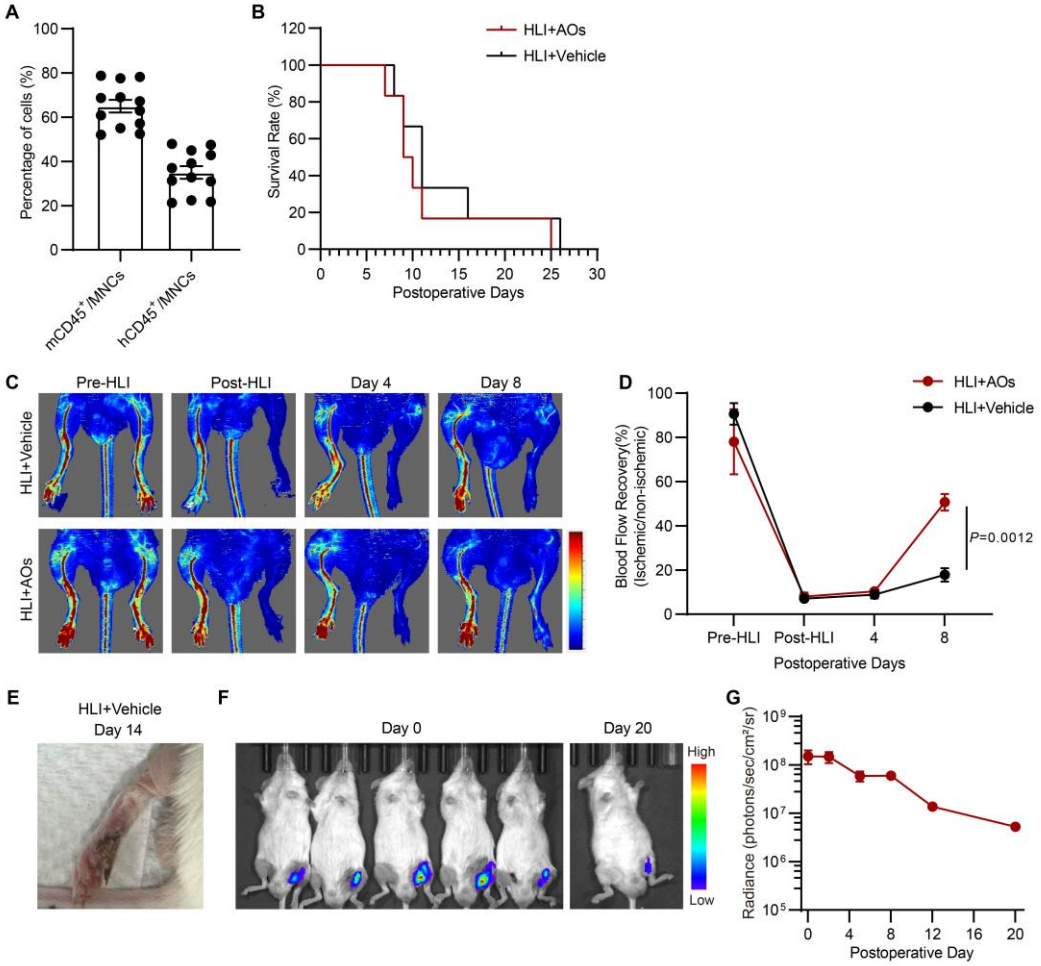

Figure S8. Evaluation of AO transplantation in a humanized hindlimb ischemia model. (**A**) Flow cytometric assessment of human immune cell reconstitution in Hu-PBMC-NPG mice prior to hindlimb ischemia induction, showing the proportions of human and mouse CD45⁺ cells among circulating mononuclear cells, *n* = 12 mice. (**B**) Kaplan–Meier survival analysis of humanized mice after hindlimb ischemia and transplantation with vehicle or AOs. (**C**) Representative Laser Doppler perfusion images of ischemic hindlimbs from vehicle- and AOs-treated humanized mice. (**D**) Quantification of blood perfusion recovery following treatment, *n* = 6 mice. Two-way ANOVA with Bonferroni post-hoc test was performed. (**E**) Representative photographs

showing progression of ischemic limb injury in humanized mice. (**F**) Representative bioluminescence images of transplanted AOs after implantation into humanized mice. (**G**) Quantification of bioluminescence signal intensity over time following AOs transplantation. Data are presented as mean ± s.e.m. Significance is indicated as n.s., not significant; **P* < 0.05; ***P* < 0.01; and ****P* < 0.001. Source data, including exact *P* values, are provided in the Source Data file.